Krystyn PAWLUK

EXACT SOLUTIONS OF INTEGRALS TO BE USED IN COMPUTING THE MAGNETIC FIELD BY BOUNDARY-INTEGRAL TECHNIQUE

ABSTRACT *Exact analytical formulae suitable to integrate the boundary quantity over a rectangular boundary element are given. They can be used in algorithms of the boundary-integral technique when some field quantity at the vicinity of the boundaries is searched for. The special computer test software was accomplished which enabled to compare the approximate integrations by Gauss quadrature to those ones obtained by the exact formulae. The error of the numerical approach increases significantly when a distance of field points from the boundary element becomes comparable with the size of it. For the larger distance, both kind of integration are equivalent. The above statement seems to be important when the boundary-integral technique should be applied to compute the magnetic field within the air gap of electric machines.*

Keywords: *magnetic field, boundary element method*

Prof. Krystyn PAWLUK
e-mail: pawluk@iel.waw.pl

Department of Electric Machines
Electrotechnical Institute

PROCEEDINGS OF ELECTROTECHNICAL INSTITUTE, Issue 241, 2009

1. INTRODUCTION

A concept of the paper corresponds to the general idea pertaining to engineering design to exploit analytical integrals, if they exist in relevant case, instead of apply approximate numerical calculations. Nowadays, the advanced mathematical procedures are used in order to solve problems of electric and magnetic fields in electrical devices. Such measures are formed into compact set of algorithms and arranged as special computer software. Boundary-integral approach or its practical accomplishment: the boundary element method (BEM), are largely known and widely applied, see for instance Kost [7], Krajewski [8], Sikora [11]. Operations of integration form the issue part of mathematical algorithms of this approach. Generally, approximate integrals are used in the algorithms, but it involves some kind of numerical inconveniences. The special procedures were searched for performing effective integration, e.g. the symbolic computation see Almeida & Pina [1], but it has not resolved the crucial difficulties of the problem, mainly related to non-singular and quasi-singular integrals.

We would like to present our consideration on the integral problems in relation to the indirect variant of the boundary-integral approach that is based on a concept of the fictitious single layer boundary quantity σ of surface density feature. Generally, this quantity is supposed to be appeared upon same part Γ_1 of the total boundaries Γ. This quantity involves the potential φ for which the basic equation holds:

$$\varphi(P) = \int_{\Gamma_1} \mathrm{G(Q,P)}\,\sigma\,\mathrm{dQ} \tag{1}$$

where the kernel $\mathrm{G(Q,P)} = \dfrac{1}{4\pi\left|\boldsymbol{R}_{\mathrm{QP}}\right|}$ is Green function in 3-D, and $\boldsymbol{R}_{\mathrm{QP}}$ is vector[1)] directed from the source point Q on Γ_1 to field point P. In a region where the potential exists, the vector field quantity (of field-strength character) can be considered, for which the following equation with relevant kernel is valid:

$$\boldsymbol{V} = -\mathrm{grad}\,\varphi = \int_{\Gamma_1} \frac{\boldsymbol{R}_{\mathrm{QP}} \cdot \sigma}{4\pi\left|\boldsymbol{R}_{\mathrm{QP}}\right|^3}\,\mathrm{dQ} \tag{2}$$

The boundary-integral approach and, in particular, the BEM represent in fact a consistent set of algorithms to deal with a set of simple boundary

[1)] $\boldsymbol{R}_{\mathrm{QP}}$ is defined by vector difference between the position vectors of point P and Q.

elements, preferably of rectangular shape, on which the above boundary quantity σ is attributed. The boundaries are practically formed as an interface between two pieces of various physical characteristics, for instance between an air and ferromagnetic core. An appropriate subdivision of the boundary to obtain a finite number of boundary elements determines a rang of matrix to be solved. Generally, the more the boundary elements are chosen, the higher accuracy of a computed field quantity is expected, however, on the other hand, the matrix rank cannot be excessively extended. The error of computed field quantity is increased at the field points situated in the vicinity of the boundaries and this problem was thoroughly examined, see for instance Igarashi & Honma [6] in relation to the magnetic field. For this reason, the boundary-integral technique seems to be hardly appropriate to compute the field within small-size air gaps, for instance in the air gap of electric machines. An example related to an idea how that problem might be treated was presented in past by Bill and co-authors [4].

It will be shown in the paper that the difficulties related to computing the magnetic field near to boundary elements and on the boundary elements itself can be effectively limited when some numerical integrations going on the typical boundary-integral algorithms are replaced by the exact formulae.

2. INTEGRALS OVER THE BOUNDARY ELEMENT

Integrations over the boundary elements are a key problem of the boundary-integral algorithms. They must be twice applied: firstly, when the matrix elements has to be calculated, and secondly, after a solving the main matrix equation, in order to compute the distribution of the field quantity that is just searched for.

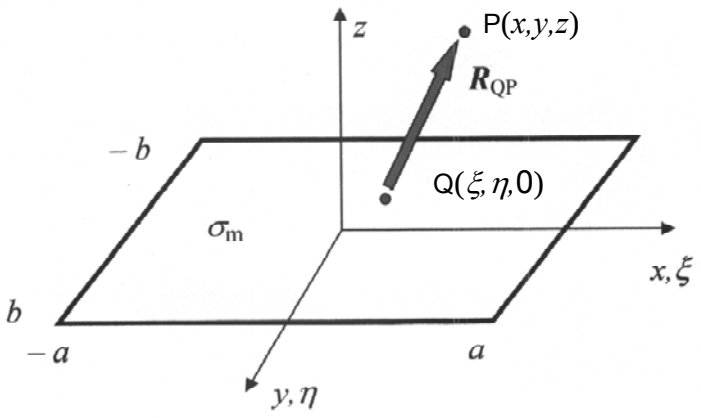

Fig. 1. Rectangular boundary element

Let us evaluate the problem of computation error when the field point approaches significantly to the boundary element. Consider the rectangle boundary element shown in figure 1.

To refer to an engineering object, suppose, not losing generality of the consideration, that the element shown in figure 1 is situated on a pole surface of a permanent magnet. Consider the magnetic flux density in the neighborhood of the magnet pole. Let the boundary quantity σ_m, that we term *surface density of magnetic charge*, see [9], and that is defined as equal to magnitude of the magnetic polarization inside the magnet, be constant over the element. Thus, at the field point P(x, y, z) situated outside the boundary, the magnetic scalar potential involved by σ_m fulfils the equation:

$$\psi_\mathrm{m}(x,y,z) = \frac{\sigma_\mathrm{m}}{4\pi\mu_0} \int_{-b}^{b} \int_{-a}^{a} \frac{1}{\left[(x-\xi)^2 + (y-\eta)^2 + z^2\right]^{1/2}} \mathrm{d}\xi\, \mathrm{d}\eta \tag{3}$$

where the denominator of the integrand is formed by the magnitude $\left|\boldsymbol{R}_\mathrm{QP}\right|$ of the vector $\boldsymbol{R}_\mathrm{QP}$. The magnetic flux density $\boldsymbol{B}$ at P(x, y, z) being generally defined by μ_0 times minus gradient of ψ_m is expressed by the formula:

$$\boldsymbol{B}(x,y,z) = \frac{\sigma_\mathrm{m}}{4\pi} \int_{-b}^{b} \int_{-a}^{a} \frac{\boldsymbol{i}(x-\xi) + \boldsymbol{j}(y-\eta) + \boldsymbol{k}z}{\left[(x-\xi)^2 + (y-\eta)^2 + z^2\right]^{3/2}} \mathrm{d}\xi\, \mathrm{d}\eta \tag{4}$$

where $\boldsymbol{i}, \boldsymbol{j}, \boldsymbol{k}$ are base vectors attributed to the local Cartesian coordinates of the boundary element.

In a professional BEM software, integrals of type (3) and (4) are mainly calculated numerically, in practice the Gauss quadrature formula is employed. The integrants of both expressions are function of two variables ξ, η for which the following abscissas are chosen $\xi_i = a\,U_i$; $y_j = b\,U_j$, where U_i and U_j are roots of the Legendre polynomial of the $N + 1$ degree to which the weights W_i and W_j. correspond. Thus, integrals (3) and (4) can be approached to the double sums:

$$\psi_\mathrm{m}(x,y,z) = \frac{ab\sigma_\mathrm{m}}{4\pi\mu_0} \sum_{i=1}^{N+1} \sum_{j=1}^{N+1} \frac{1}{\left|(x-\xi_i)^2 + (y-\eta_j)^2 + z^2\right|^{1/2}} \cdot W_i \cdot W_j \tag{5}$$

$$\boldsymbol{B}(x,y,z) = \frac{ab\sigma_\mathrm{m}}{4\pi} \sum_{i=1}^{N+1} \sum_{j=1}^{N+1} \frac{\boldsymbol{i}(x-\xi_i) + \boldsymbol{j}(y-\eta_j) + \boldsymbol{k}z}{\left[(x-\xi_i)^2 + (y-\eta_j)^2 + z^2\right]^{3/2}} \cdot W_i \cdot W_j \tag{6}$$

We intend to show that it is useful, for the rectangular boundary element, to employ the exact integral formulae of (3) and (4) instead of (5) and (6).

3. MAGNETIC FLUX DENSITY

Basic solution

Let us start up the consideration from formula (4) because the exact solution in this case is relatively simpler than that one of formula (3). Following the Ryshik and Gradstein tables [10], we have shown in [9] that the exact solution of double integral (4) can be reached explicite[2)].The following formulae for the particular coordinates of $\boldsymbol{B}$ hold:

$$B_x(x,y,z) = \frac{\sigma_m}{8\pi}\left(\ln w_1 - \ln w_2 - \ln w_3 + \ln w_4\right) \tag{7}$$

$$B_y(x,y,z) = \frac{\sigma_m}{8\pi}\left(\ln v_1 - \ln v_2 - \ln v_3 + \ln v_4\right) \tag{8}$$

$$B_z(x,y,z) = \frac{\sigma_m}{4\pi}\left(\arctan u_1 - \arctan u_2 - \arctan u_3 + \arctan u_4\right) \tag{9}$$

where the arguments w, v, u being functions as well of size a and b of the rectangle boundary element as of coordinates x, y, z of point P are given below:

$$w_{1,2} = \frac{(y+b) \pm \sqrt{(x+a)^2 + (y+b)^2 + z^2}}{(y+b) \pm \sqrt{(x-a)^2 + (y+b)^2 + z^2}} \quad ; \quad w_{3,4} = \frac{(y-b) \pm \sqrt{(x+a)^2 + (y-b)^2 + z^2}}{(y-b) \pm \sqrt{(x-a)^2 + (y-b)^2 + z^2}}$$

$$v_{1,2} = \frac{(x+a) \pm \sqrt{(x+a)^2 + (y+b)^2 + z^2}}{(x+a) \pm \sqrt{(x+a)^2 + (y-b)^2 + z^2}} \quad ; \quad v_{3,4} = \frac{(x-a) \pm \sqrt{(x-a)^2 + (y+b)^2 + z^2}}{(x-a) \pm \sqrt{(x-a)^2 + (y-b)^2 + z^2}}$$

$$u_{1,2} = \frac{(x+a)(y \pm b)}{z\sqrt{(x+a)^2 + (y \pm b)^2 + z^2}}; \qquad u_{3,4} = \frac{(x-a)(y \pm b)}{z\sqrt{(x-a)^2 + (y \pm b)^2 + z^2}}$$

For a compact form of formulae (7)-(9) see Amendment.

[2)] Two exact solutions of indefinite integrals No. 2.264.5 and 2.284 given in [10] were applied, consecutively, with the integral limits as well.

Singular integral at the centre of element

We would like to present the following procedure to determine B_z at the centre of the rectangular boundary element carrying σ_m = const. When point P tends to any point localized upon the boundary element the kernel of integral (4) tends to infinity and the integral becomes singular. To determine its value for P(0, 0, 0), the following treatment is proposed. Let us rewrite the above arguments related to P(0, 0, ε). Substituting x = 0 and y = 0 we have all arguments w and v equal to 1 for any ε. The above results in disappearing of all natural logarithms, thus equations (7) and (8) give correctly zero for the components B_x and B_y.

The following procedure leads to determine the component B_z. The arguments u for the point P(0; 0; ε) are:

$$u_1 = u_4 = \frac{ab}{\varepsilon\sqrt{a^2+b^2+\varepsilon^2}}; \quad u_2 = u_3 = \frac{-ab}{\varepsilon\sqrt{a^2+b^2+\varepsilon^2}} = -u_1$$

and equation (9) can be simplified to read:

$$B_z(0,0,\varepsilon) = \frac{\sigma_m}{4\pi} 2\left(\arctan u_1 - \arctan(-u_1)\right) = \frac{\sigma_m}{4\pi} 2\left(\pi + \arctan\frac{2u_1}{1-u_1^2}\right). \quad (9a)$$

where the formula of a difference between two inverse tangents for the respective arguments $u_1 > 1$ and $-u_1 < -1$ was applied.

For $\varepsilon \to 0$ the argument $u_1 \to \infty$ thus $\lim_{u_1\to\infty} \arctan\frac{2u_1}{1-u_1^2} = 0$, hence the singular value of the magnetic flux density at the centre of boundary element is as follows:

$$\boldsymbol{B} = \boldsymbol{k} B_z(0,0,0) = \boldsymbol{k}\frac{\sigma_m}{2} \quad (9b)$$

being dependent neither on a nor on b.

Test calculations

A special test software[3)] was developed with intention to compare the results of approximate integration by Gauss quadrature (6) to those ones

[3)] Program BEM_B.

of exact formulae (7)-(9). All computed results that are presented by the following figures are related to the boundary element 2a x 2b = 10 mm x 10 mm and to the boundary quantity σ_m = 1 T supposing to be uniformly distributed upon the surface of the boundary element. The magnetic flux density due to σ_m is computed lengthways the field-point segment $P_1 - P_2$ that can be traced anywhere, outside the boundary surface.

The computed results shown in figure 2 concern the segment coinciding with z-axis, hence, only the B_z components exist. The exact integration was performed accordingly to formulae (7)-(9) and similarly the numerical integration, i.e. the double Gauss quadrature corresponding to Legendre polynomial of degree N + 1 = 4 was applied (i.e. 16 abscissas upon the element are considered). One can observe that the discrepancy between two curves has a significant value at distance of 0,5 mm from the boundary. It decreases at longer distances and disappears, almost entirely, at distance about 3,5 mm. Over this value both curves coincide. The test calculation for N + 1 = 6 (36 abscissas) does not give a sufficient improvement on the matter. Curve 1 representing the exact integration tends evidently to the singular value of B_z which, in conformity with (9b) and for σ_m = 1 T, is equal to $\sigma_m/2 = 0{,}50$ T.

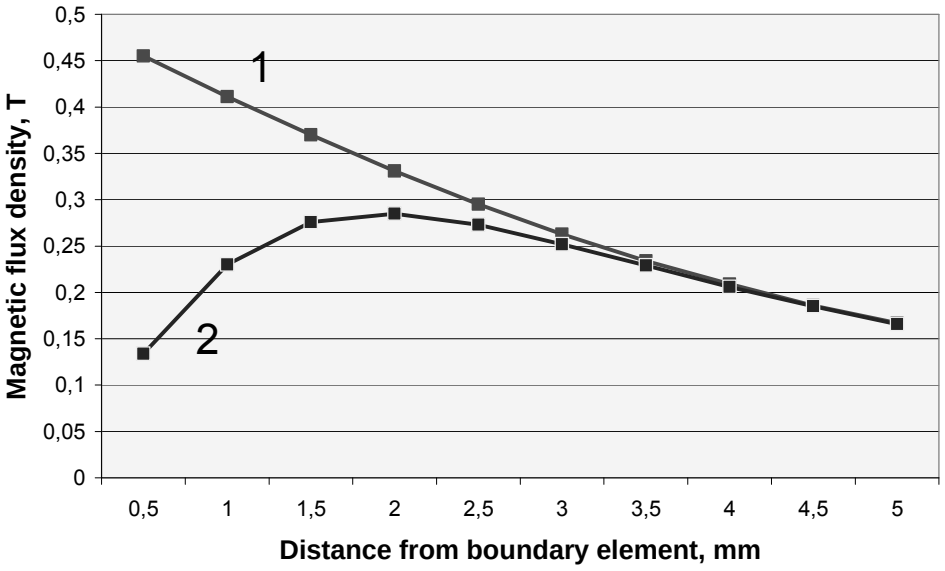

Fig. 2. Magnetic flux density lengthways the segment P_1(0,0; 0,0; 0,5) – P_2(0,0; 0,0; 5,0)
1 – Exact integration, 2 – Numerical integration (double Gauss quadrature formula)

The curves shown in figure 3 are related to the segment of the field points laying on the line perpendicular to the boundary element, and crossing it at point P_1(2,5; 2,5; 0,0) i.e. at ¼ of the diagonal of the element. The computed field represents a magnitude of vector $B = |\boldsymbol{B}|$ having in this case all three non-zero components that were calculated, separately. The discrepancy between the curves calculated by the exact formulae and by the numerical ones is also observed; it disappears about the similar distance as in the case of figure 2, however, the numerical calculation results in this case in higher values that the corresponding exact results, inversely than in previous case.

The curves in figure 4 differ from those of two previous figures on the field-points segment position that coincides with the line crossing the boundary element just at its corner. We observe that the numerical and exact calculations differ slightly each other and this small discrepancy disappears at 2,5 mm from the element surface. The similar calculation performed for the line with pole-points segment crossing the element surface outside the element itself shown the results of the numerical calculation that coincide, even in the vicinity of this surface, with the results of exact calculation.

The results of the exact and numerical integrations pertaining to the component B_x at points situated lengthways the segment $P_1 – P_2$ parallel to x axis and 1,0 mm distant from the boundary element surface, and traced from x = 0 till to x = 2a is shown in figure 5. The values calculated by exact integration (curve 1) mark the function $B_x(x)$ being quite linear over the element but hyperbolic outside of it. The results of the numerical integration (curve 2) show irregular distributions over the element but out of the element it becomes like curve 1, exactly. Such irregularity is increased for similar $P_1 – P_2$ segments situated nearly the element, and disappears for segments at distance over 3,0 mm from the element.

The dependence of the shape of curve $B_z(z)$ upon the size of the boundary element, for z taking values from z = 0,0 mm till to z = 5,0 mm is illustrated in figure 6. The value $B_z(0)$, see formula (9b) for its singular value, is independent on size of the rectangular element and (for σ_m = 1 T) it is equal to 0,5 T for each of the considered boundary element . For z > 0, a shape of the curves is affected by the element size. The minor is the element, the substantial is deflection of the curves from their initial values.

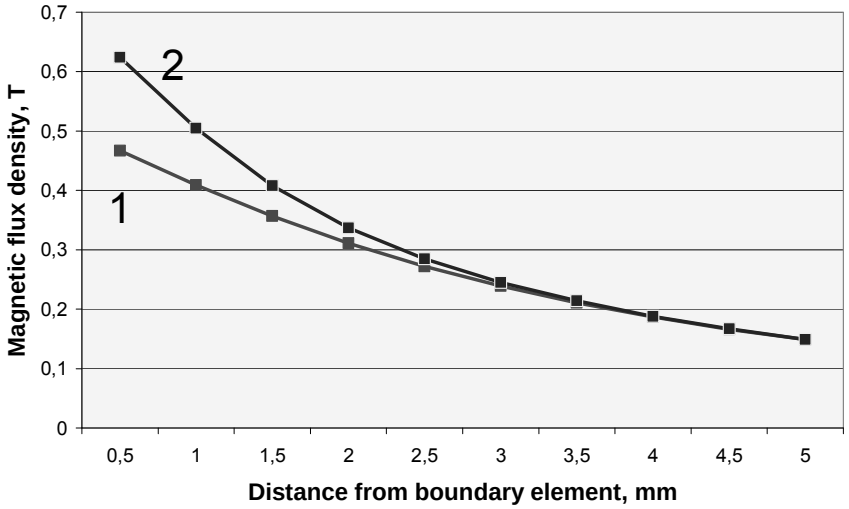

Fig. 3. Magnetic flux density lengthways the segment P_1(2,5; 2,5; 0,5) – P_2(2,5; 2,5; 5,0)
1 – Exact integration, 2 – Numerical integration (double Gauss quadrature formula)

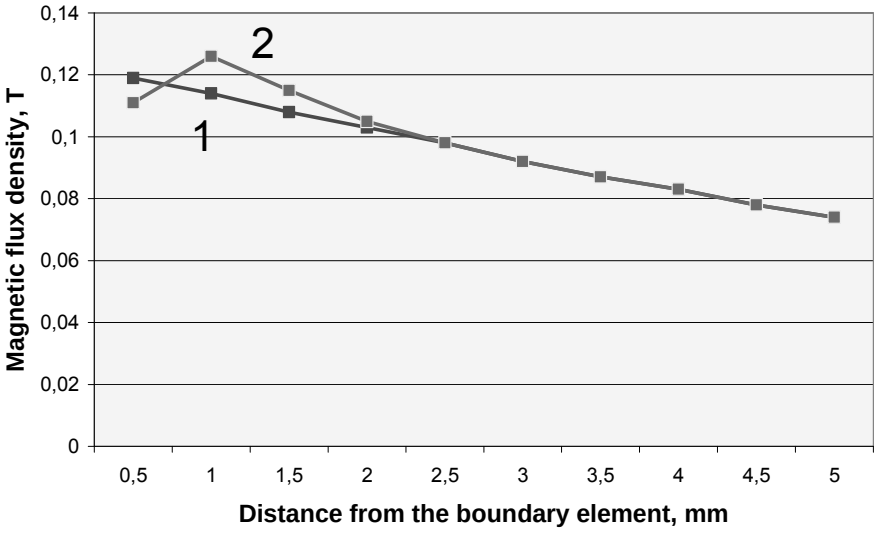

Fig. 4. Magnetic flux density lengthways the segment P_1(5,0; 5,0; 0,5) – P_2(5,0; 5,0; 5,0)
1 – Exact integration, 2 – Numerical integration (double Gauss quadrature formula)

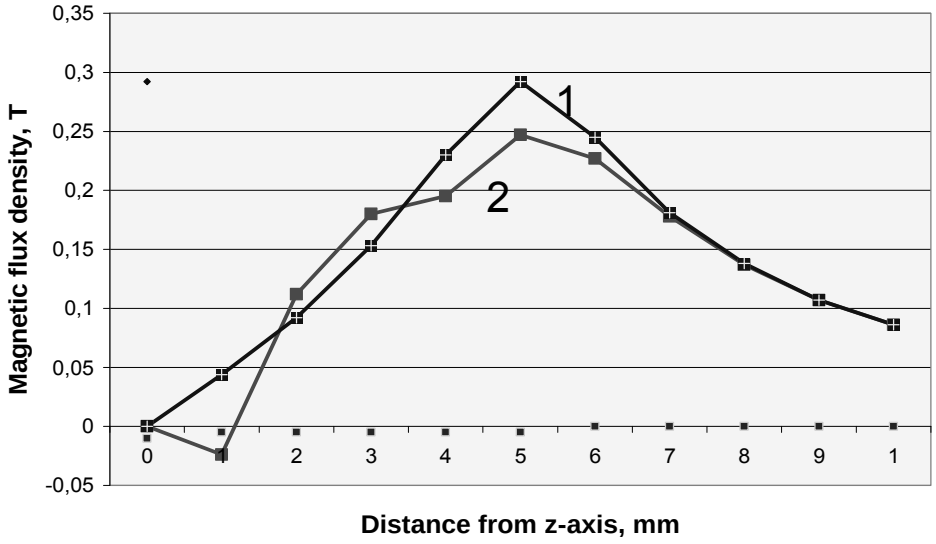

Fig. 5. Component B_X of magnetic flux density lengthways the segment $P_1(0,0; 0,0; 1,0) – P_2(10,0; 0,0; 1,0)$
1 – Exact integration, 2 – Numerical integration (double Gauss formula)

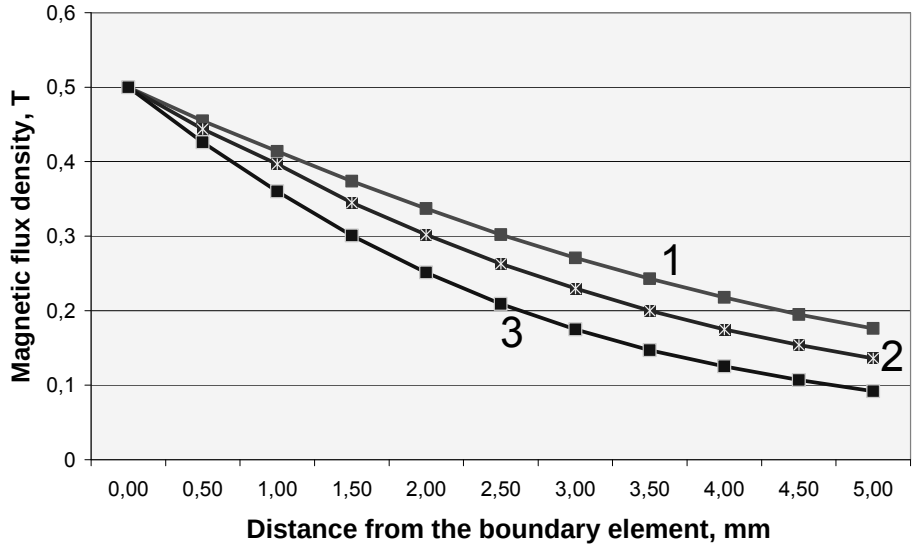

Fig. 6. Magnetic flux density lengthways the segment $P_1(0,0; 0,0; 0,0) – P_2(0,0; 0,0; 5,0)$ of various boundary elements: 1) 10 mm x 10 mm, 2) 8 mm x 8 mm, 3) 4 mm x 4 mm

4. MAGNETIC SCALAR POTENTIAL

Basic solution

The formula of the scalar magnetic potential (3) can be easy integrated only with respect to one source variable. The integration with respect to η gives[4)] the following two-term formula:

$$\psi_{\mathrm{m}}(x,y,z)=\frac{\sigma_{\mathrm{m}}}{4\pi\mu_0}\int_{-b}^{b}\left[\operatorname{sh}^{-1}\frac{x+a}{\sqrt{(y-\eta)^2+z^2}}-\operatorname{sh}^{-1}\frac{x-a}{\sqrt{(y-\eta)^2+z^2}}\right]\mathrm{d}\eta \qquad (11)$$

Taking regard that the inverse hyperbolic sine is joint with the natural logarithm by the obvious equation:

$$\operatorname{sh}^{-1}u=\ln\left(u+\sqrt{u^2+1}\right) \qquad (12)$$

the compact formula of (11) can be equivalently read as follows:

$$\psi_{\mathrm{m}}(x,y,z)=\frac{\sigma_{\mathrm{m}}}{4\pi\mu_0}\int_{-a}^{a}\left[\ln\frac{y+b+\sqrt{(x-\xi)^2+(y+b)^2+z^2}}{y-b+\sqrt{(x-\xi)^2+(y-b)^2+z^2}}\right]\mathrm{d}\xi \qquad (11a)$$

but both (11) and (11a) rise problems of their further (with respect to ξ) exact integration. Azis [2] has quoted some exact solution of the indefinite integral appearing in (11) and Craik [5] recalls it by a simple notice, only. In order to examine the Azis' proposal we rewrite it in developed form with the integral limits to get the formula

$$\psi_{\mathrm{m}}(x,y,z)=\frac{\sigma_{\mathrm{m}}}{4\pi\mu_0}\left(\lambda_{\mathrm{m}}^{(1)}+\lambda_{\mathrm{m}}^{(2)}+\lambda_{\mathrm{m}}^{(3)}+\lambda_{\mathrm{m}}^{(4)}\right) \qquad (13)$$

which is composed with four terms, each having three sub-terms that we give below:

[4)] See [10], integral No 2.261.

$$\lambda_{\mathrm{m}}^{(1,2)} = \pm(y+b)\,\mathrm{sh}^{-1}\frac{x\pm a}{\sqrt{(y+b)^2+z^2}} \pm(x\pm a)\,\mathrm{sh}^{-1}\frac{y+b}{\sqrt{(x\pm a)^2+z^2}} \mp z\arctan\frac{(x\pm a)(y+b)}{z\sqrt{(x\pm a)^2+(y+b)^2+z^2}}$$

$$\lambda_{\mathrm{m}}^{(3,4)} = \mp(y-b)\,\mathrm{sh}^{-1}\frac{x\pm a}{\sqrt{(y-b)^2+z^2}} \mp(x\pm a)\,\mathrm{sh}^{-1}\frac{y-b}{\sqrt{(x\pm a)^2+z^2}} \pm z\arctan\frac{(x\pm a)(y-b)}{z\sqrt{(x\pm a)^2+(y-b)^2+z^2}}$$

When the particular terms of the above are suitably assembled and arranged and yet equation (12) is applied to them, the friendly form composed with five terms Λ_{m} can be got:

$$\psi_{\mathrm{m}}(x,y,z) = \frac{\sigma_{\mathrm{m}}}{4\pi\mu_0}\left(\Lambda_{\mathrm{m}}^{(1)} + \Lambda_{\mathrm{m}}^{(2)} + \Lambda_{\mathrm{m}}^{(3)} + \Lambda_{\mathrm{m}}^{(4)} + \Lambda_{\mathrm{m}}^{(5)}\right) \tag{14}$$

where the particular terms are expressed below:

$$\Lambda_{\mathrm{m}}^{(1,2)} = (y\pm b)\,\ln\frac{x+a+\sqrt{(x+a)^2+(y\pm b)^2+z^2}}{x-a+\sqrt{(x-a)^2+(y\pm b)^2+z^2}}$$

$$\Lambda_{\mathrm{m}}^{(3,4)} = \pm(x\pm a)\,\ln\frac{y+b+\sqrt{(x\pm a)^2+(y+b)^2+z^2}}{y-b+\sqrt{(x\pm a)^2+(y-b)^2+z^2}}$$

$$\Lambda_{\mathrm{m}}^{(5)} = -z\left[\arctan u_1 - \arctan u_2 - \arctan u_3 + \arctan u_4\right]$$

where the arguments u are identical as in formula (9). For the compact form of $\Lambda_{\mathrm{m}}^{(5)}$ see Amendment.

Singular integral at the center of element

The integral (3) expressing the magnetic scalar potential at points P localized upon the boundary element is singular. Let us examine the problem for the point P(0, 0, ε) tending to the centre of the element. Notice, referring to

the exact solution of ψ_m given by formula (14), that the first four terms exist at P(0,0,0) and they are, after substituting x = 0, y = 0 and $\varepsilon \to 0$, to read:

$$\Lambda_{m0}^{(1)} + \Lambda_{m0}^{(2)} = 2b \ln \frac{\sqrt{a^2+b^2}+a}{\sqrt{a^2+b^2}-a} \; ; \; \Lambda_{m0}^{(3)} + \Lambda_{m0}^{(4)} = 2a \ln \frac{\sqrt{a^2+b^2}+b}{\sqrt{a^2+b^2}-b} \qquad (15)$$

To determine the last term $\Lambda_{m0}^{(5)}$ at this point, note that the above substitution leads to:

$$\Lambda_{m}^{(5)}(0,0,\varepsilon) = 2\varepsilon \left[\arctan \frac{-ab}{\varepsilon\sqrt{a^2+b^2+\varepsilon^2}} - \arctan \frac{ab}{\varepsilon\sqrt{a^2+b^2+\varepsilon^2}} \right]$$

and we have, applying the formula for a difference of two inverse tangent functions that was used in previews chapter, that $\Lambda_{m0}^{(5)} = \lim_{\varepsilon \to 0} 2\varepsilon \, \pi = 0$, hence, the sum of the only four members (15) determines the magnetic scalar potential at the center of the rectangular boundary element with uniformly distributed σ_m to read:

$$\psi_m(0,0,0) = \frac{\sigma_m}{4\pi\mu_0} \left(\Lambda_{m0}^{(1)} + \Lambda_{m0}^{(2)} + \Lambda_{m0}^{(3)} + \Lambda_{m0}^{(4)} \right) \qquad (14a)$$

Test calculations

The author has accomplished a specialize test software[5)] in order to examine the above solutions. The results of the performed computation are presented in figure 7. The field-point segment is chosen on z-axis similarly as it was done for calculated results of B_z presented in figure 2. Curve 1 gives the result of exact solution – formula (13) , curve 2 represents the results obtained by applying the single Gauss quadrature formula to equation (10), in relation to the variable ξ; curve 3 gives results of full-numerical integration by the double Greens formula with respect to both source variables, equation (5). The discrepancies between the curves are observed at distance till to 2 mm from the boundary element, and moreover, they are relatively smaller than we have observed for the magnetic flux density, compare figure 2. Generally, a correctness attainted by the exact formula seems be principally better. Curve 1 is quite

[5)] Program BEM_PSI

monotonic that corresponds to physical character of the potential. It is not the case of curves 2 or 3. For $z \to 0$, curve 1 tends to value 0,223 kA that results from formula (14a) related to the singular solution of equation (3). It is not the case for the approximate solutions.

The practical correctness of values of ψ_{m} computed by the exact formula can be verified by comparison the magnetic flux density $B_{\mathbf{z}}$ calculated by exact formula (9) with its value expressed by $-\mu_0 \operatorname{grad}_z \psi_{\mathrm{m}}$. Consider for instance the value of B_z at point P(0,0; 0,0; 1,5) at z-axis. It is equal to 0,370 T, see Fig. 2. If we approximate the $\operatorname{grad}_z \psi_{\mathrm{m}}$ by its final difference of two values of ψ_{m} given in figure 7 that correspond to points P(0,0; 0,0; 1,0) and P(0,0; 0,0; 2,0) we get:

$$B_z = -\mu_0 \frac{\psi_{\mathrm{m}}(0{,}0;\, 0{,}0;\, 1{,}0) - \psi_{\mathrm{m}}(0{,}0;\, 0{,}0;\, 2{,}0)}{2{,}0\text{-}1{,}0} = -\mu_0 \frac{1{,}576 - 1{,}87}{1{,}0} = 0{,}369 \text{ T}$$

that verifies the coincidence of the both exact formulae: of the magnetic flux density (9) and the scalar magnetic potential (13)[6]. A small difference of the last digits is result of fact that formula (9) giving the value of 0,370 T is obtained by exact differentiation the ψ_{m} with respect to z, but the value of 0,369 T is calculated by final difference procedure, thus by an approximate calculation.

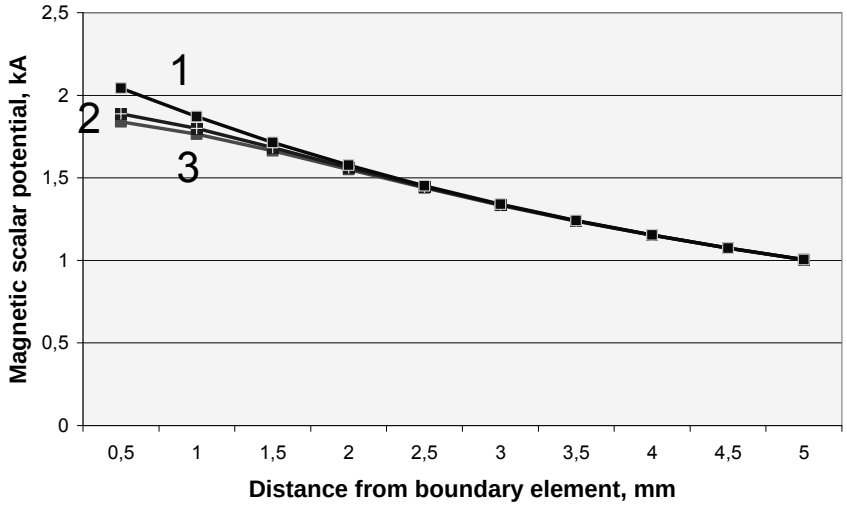

Fig. 7. Magnetic scalar potential lengthways segment P_1(0,0; 0,0; 0,5) – P_2(0,0; 0,0, 5,0)
1 – Exact integration, 2 – Half-numerical integration (single Gauss quadrature formula), 3 – Full numerical integration (double Gauss quadrature formula)

[6] For all calculations referred in the paper, the following units, coherent each other, are applied: for length mm, for magnetic flux density T, for scalar magnetic potential kA, and for magnetic constant μ_0 = 0,4 π kH/mm.

Figure 8 shows the results of computation the magnetic scalar potential ψ_m lengthways the segment $P_1 - P_2$ traced paralleling to x-axis and 1 mm distant from the surface of element (the computed component B_x corresponding to this segment is shown in figure 6). Over the boundary element, the particular curves 1, 2 and 3 differ each other but not so far as curves of B_x corresponding to them, however, curve 1 representing the exact integration is monotonic and it has the most regular shape. In the region outside the element all three curves have almost hyperbolic shape and they become identical.

Similarly, as we have shown that in the case of component B_z the correctness of B_x can be testified. Let us observe that formula (7) gives $B_x = 1{,}153$ T at P(3,0; 0,0; 1,0). On the other hand we get from formula (13) that $\psi_m = 1{,}799$ kA at P(2,0; 0,0; 1,0) and $\psi_m = 1{,}552$ kA at P(4,0; 0,0; 1,0), thus, applying the final difference of ψ_m with respect to x, we obtain $B_x(3{,}0; 0{,}0; 1{,}0) = 1{,}155$ T. It verifies accuracy of both exact formulae, at least till to the third digit; a difference of the fourth digits is due to small inaccuracy of final difference if compared with the exact differentiation with respect to x.

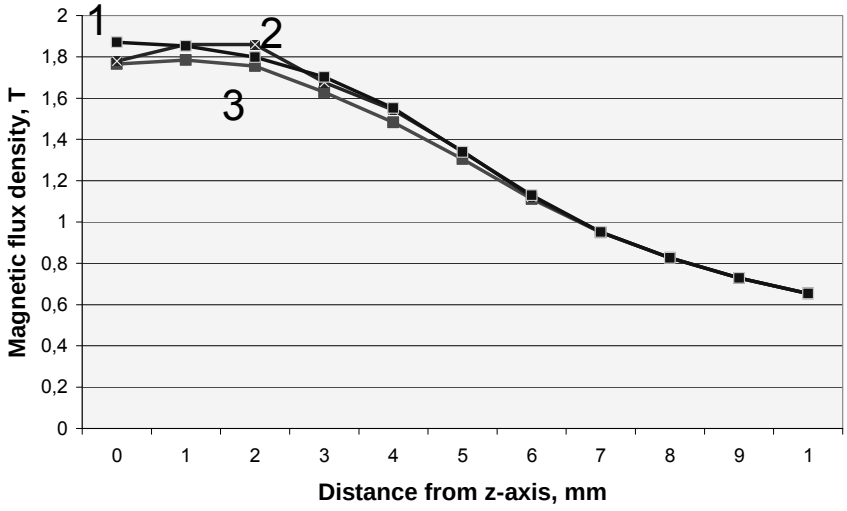

Fig. 8. Magnetic scalar potential lengthways segment P_1(0,0; 0,0; 1,0) – P_2(10,0; 0,0, 1,0)
1 – Exact integration, 2 – Half-numerical integration (single Gauss quadrature formula), 3 – Full numerical integration (double Gauss quadrature formula

5. CONCLUSIONS

The exact analytical solutions of the surface integrals over a rectangle boundary element that are preferred for the boundary-integral algorithms are

presented in the paper. The particular solutions pertaining to the magnetic field due to permanent magnet were presented in sense of an example of the potential field treated by such approach. The results of exact integration were compared with that ones obtained by approximate numerical integration.

It is proved that in the vicinity of the boundary element the approximate integrals leads to evident inaccuracy. As well the scalar quantities of potential type as the vector quantities determined by their gradients are concerned. The above statements pertains, generally, to a region that is distanced from a boundary element less than a size of the element itself.

The exact integral formulae presented in the paper were effectively applied in a special software intended for computing the magnetic flux distribution within an air gap of an electric generator with permanent magnet field system.

The main suggestions issued from the main consideration presented in the paper are the following. When the algorithms based on the boundary-integral technique should be accomplished the kind of integration technique applied in them should be well thought-out. Although the boundary-integral algorithm operates with the boundary elements of rectangular shape and, moreover, the constant-value boundary quantity is supposed to be distributed upon the element then the exact analytical solutions of the integral over the boundary elements could be introduced into the algorithms. The analytical solutions given in the paper take practically exact results that are independent on the distance of the field points from the boundary elements. Moreover, when the field points are localized on the boundary itself and the relevant integrals becomes singular the exact integral formulae, when submitted to a limit procedure, lead to analytical solutions of the singular integrals, too. The use of the exact analytical integrals is not necessary for the field point localized at distance from the boundary element larger than the size of the element, where the numerical integrals may be applied as well.

Amendment

In computer software equations (7) and (8) should be coded in compact form:

$$B_x(x,y,z) = \frac{\sigma_{\mathrm{m}}}{8\pi} \ln \frac{w_1 w_4}{w_2 w_3} \tag{7c}$$

$$B_y(x,y,z) = \frac{\sigma_{\mathrm{m}}}{8\pi} \ln \frac{v_1 v_4}{v_2 v_3} \tag{8c}$$

Equation (9) can be also compactly coded, however, some conditions related to the values of the arguments u shall be checked up, thus

$$B_z(x,y,z) = \frac{\sigma_{\mathrm{m}}}{4\pi}\left[\left(\arctan\frac{u_1-u_2}{1+u_1u_2}+k\pi\right)-\left(\arctan\frac{u_3-u_4}{1+u_3u_4}+l\pi\right)\right] \qquad (9c)$$

where the parameter k obeys the following conditions:

- if $u_1u_2 > -1$ then $k = 0$,
- if $u_1u_2 < -1$ and $u_1 > 0$ then $k = 1$,
- if $u_1u_2 < -1$ and $u_1 < 0$ then $k = -1$.

The similar conditions concern the parameter l in dependence on u_3 and u_4. The formula of the 3-rd term of magnetic scalar potential $\lambda_{\mathrm{m}}^{(3)}$ appearing in equation (14) can be identically transformed into the compact form to read:

$$\Lambda_{\mathrm{m}}^{(5)} = -z\cdot\left[\left(\arctan\frac{u_1-u_2}{1+u_1u_2}+k\pi\right)-\left(\arctan\frac{u_3-u_4}{1+u_3u_4}+l\pi\right)\right]$$

with the conditions for k and l quite identical as in equation (9c).

LITERATURE

1. Almeida A., Pina H.L. The solution of boundary problems using symbolic computation, Boundary Element Technology VIII, ed. Pina H. & Brebbia C.A. Computational Mechanics Publications, Southampton, Boston, pp. 289-301, 1993.
2. Azis. Z., Thesis, Manchester University, 1978.
3. Babic S., Akyel C., Gavrilović M.M., Calculation improvement of 3D linear magnetostatic field based on fictitious magnetic surface charge, IEEE Trans. on Magnetics, Vol. 36, No. 5, pp. 3125-3127, 2000.
4. Bill K, Pawluk K., Perzanowski W., Coupling of the finite element and boundary element methods by iterative technique, Electromagnetic Fields in Electrical Engineering, ed. by Savini A. & Turowski J., Plenum Press, new York, London, pp. 187-192, 1988.
5. Craik D., Magnetism, principles and applications, John Willey & Sons, New York, 1995.
6. Igarashi H., Honma T., A boundary-element analysis of magnetic fields near surfaces, Boundary Element Technology VIII, ed. Pina H. & Brebbia C.A. Computational . Mechanics Publications, Southampton, Boston, pp. 157-166, 1993.
7. Kost A., Numerische Methoden in der Berechnung elektromagnetischer Felder, Springer Verlag, 1994.

8. Krajewski W., Elementy brzegowe i liniowe w analizie wybranych zagadnień EMC niskiej częstotliwości, Prace Instytutu Elektrotechniki, Vol. 52, No. 224, 2005.
9. Pawluk K., Permanent magnet field calculated by the boundary-integral approach. Arch. of Electrical Engineering, Vol. 57, No. 3-4, pp. 257-276, 2008.
10. Ryshik I.M., Gradstein I.S., Tables of series, products and integrals, VEB Deutscher Verlag der Wissenschaften, Berlin, 1957.
11. Sikora J., Boundary element method for impedance and optical tomography, Oficyna Wydawnicza Politechniki Warszawskiej 2007.

Manuscript submitted 21.04.2009
Reviewed by Prof. Jan Sikora

ANALITYCZNE WZORY CAŁKOWE DO STOSOWANIA W OBLICZENIACH WIELKOŚCI POLOWYCH TECHNIKĄ CAŁEK BRZEGOWYCH

K. PAWLUK

STRESZCZENIE *Podano dokładne wzory do całkowania wielkości brzegowej po prostokątnym elemencie brzegowym. Mogą one znaleźć zastosowanie w algorytmach technik całkowo-brzegowych, gdy obliczenie dotyczy wielkości polowych w pobliżu samego elementu brzegowego. Specjalnie przygotowane testowe programy komputerowe umożliwiły przeprowadzenie porównań wyników obliczeń całkowania przeprowadzonego numerycznie kwadraturą Gaussa z całkowaniem za pomocą podanych wzorów analitycznych. Błąd obliczenia numerycznego wzrasta znacząco dla punktów polowych, gdy ich odległość od elementu brzegowego staje się współmierna z rozmiarem samego elementu. Dla większych odległości obydwa rodzaje całkowania są równoważne. Powyższe stwierdzenie jest szczególnie istotne, gdy technika całkowo-brzegowa ma być zastosowana do obliczania pola magnetycznego w szczelinie powietrznej maszyny elektrycznej.*

Prof. Krystyn PAWLUK was born in 1926; he received the M.Sc. and El. Eng. (1951), and later the Ph.D. degree from the University of Mining and Metallurgy in Cracow. He became habilitation from the Electrotechnical Institute in Warsaw (1974) and the title of professor in 1979.

In 1951…1961 – assistant-professor at the Department of Electric Machines in the University of Mining and Metallurgy in Cracow, in 1961…1980 – research-engineer in the Department of Electric Machines in the Electrotechnical Institute in Warsaw. 1981…1983 – assistant-professor at the Institut Agronomique et Vétérinaire de l'Université de Mohammed V in Rabat, Morocco, since 1983 – professor at the Department of Fundamental Research in Electrotechnics in Electrotechnical Institute in Warsaw, at since 2004 – professor at the Department of Electric Machines in this Institute. Since 1985, prof. Pawluk has been nominated the expert of the Polish Committee of Standardization at the International Electrotechnical Commission and takes continuously part in works of IEC committees and working groups No1 – Terminology and No 25 – Quantities and Units. For this activity, prof. Pawluk was honored in 2006 by the IEC Award. He is also a president of the national technical committee of standardization for terminology and units in electrical engineering.

Prof. Pawluk develops large research activity: project leaderships, heading of laboratories, he is the author of numerous scientific works (about 150 bibliographic items), conference reports, reviewing of scientific works, opponent of doctor thesis, etc. His main research field is the following:

- electric machines, in particular synchronous machines, measurement of transient quantities, dynamic behavior and design of turbo-generators and motors,
- electric and magnetic fields in objects of electrical technology, boundary-integral technique, inverse problems, stationary and quasi-stationary fields, permanent magnets,
- terminology and units of electrical technology.